

05,09,13

Magnetization induced second harmonic generation in thin films with ferromagnet/antiferromagnet interfaces

© V.V. Radovskaia¹, A.I. Maydykovskiy¹, V.B. Novikov¹, D.A. Kopylov¹,
N.S. Gusev^{2,3}, I.Yu. Pashen'kin^{2,3}, T.V. Murzina¹

¹ Moscow State University,
Moscow, Russia

² Institute of Physics of Microstructures, Russian Academy of Sciences,
Nizhny Novgorod, Russia

³ Lobachevsky State University,
Nizhny Novgorod, Russia

E-mail: radovskaia.vv16@physics.msu.ru

Received April 29, 2022

Revised April 29, 2022

Accepted May 12, 2022

We experimentally studied the generation of optical second harmonic (SH) and magneto-optical effects at the SH frequency in thin films consisting of ferromagnetic and antiferromagnetic materials, including exchange-bonded layers, one of which is pinned with an antiferromagnetic layer. As expected, the loops of the linear magneto-optical Kerr effect are shifted relative to the zero magnetic field value, which reflects the presence of a pronounced exchange interaction in such structures. It is shown that in the case of the nonlinear Kerr magneto-optical effect this effect is also present, but it is significantly smaller than in the nonlinear case, and leads to the observation of only one hysteresis loop instead of two. The studied dependence of the magneto-optical response at the TH frequency on the probing laser radiation power demonstrates that its growth leads to a decrease in the magnetic hysteresis loop shift of the TH.

Keywords: magnetization-induced SHG, ferromagnet/antiferromagnet interface, pinned structure, thin films

DOI: 10.21883/PSS.2022.09.54177.48HH

1. Introduction

Heterostructures based on ferromagnetic (FM) and anti-ferromagnetic (AF) materials are being actively investigated due to the presence of a number of unique properties, primarily magnetoresistant ones [1–5], and the wide possibilities of their practical use. Of great interest are the so-called pinning multilayer heterostructures in which one of the FM layers is „attached“ (pinned) due to proximity to the antiferromagnetic layer, which causes the loop of its magnetic hysteresis to shift relative to the zero value of the external magnetic field [6,7]. The magneto-resistance effect of such structures allows them to be used as spin valves [8–10]. From a fundamental point of view, it is interesting to study the magnetic and optical effects associated with non-collinear magnetization distribution in a multi-layered structure [6].

The effects in magnetic nano-heterostructures are largely determined by the properties of their partition boundaries, so the urgent task is to develop highly sensitive to interface features experimental methods for the study. These include the magneto-induced second harmonica (MISH) method, which allows the study of the magneto-optical properties of the partition boundaries [11,12], as opposed to traditional linear magneto-optic methods, characterizing the volumetric magnetic properties of the structure [13]. Note that with the help of MISH generation it is pos-

sible to investigate the exchange interaction in magnetic heterostructures, as well as to detect non-trivial states of magnetization [14–17].

The aim of this work was the experimental study of the peculiarities of magneto-induced second harmonica (MBG) generation in multilayer nanostructures with pinning and free ferromagnetic layers, as well as in ferromagnetic layer structures, bordering with para- or antiferromagnetic materials.

2. Experimental procedure

In this paper the multi-layer composition nanostructure NiFe(5)/NiCu(5)/CoFe(5)/IrMn(10)/Ta(2) on the glass substrate (brackets indicate the thicknesses of layers in nm), as well as double-layer structures of CoFe(4)/IrMn(10), NiFe(4)/IrMn(10), NiCu(10)/NiFe(10) were studied. Pinning of the CoFe bonded layer was achieved by its exchange interaction with its adjacent layer of an antiferromagnet (IrMn). Samples produced by magnetron sputtering in the atmosphere of argon at a pressure of $4 \cdot 10^{-3}$ Torr, preliminary pumping in the chamber was carried out at a pressure of up to 10^{-5} Torr, static magnetic field with a tension of about 200 Oe was applied in the film plane during the layer spraying process IrMn.

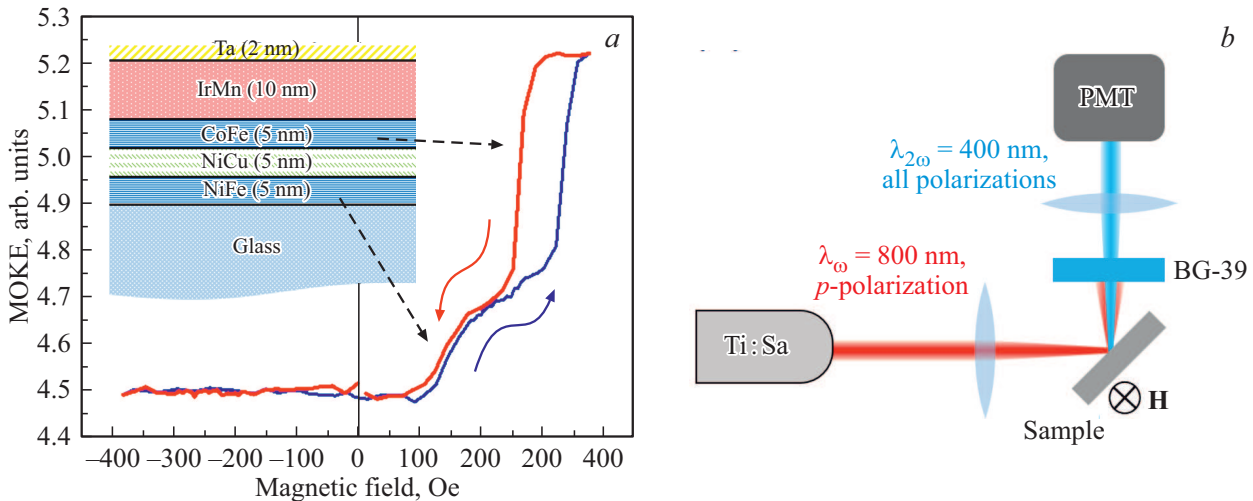


Figure 1. (a) The linear magneto-optic Kerr effect (MOKE) for NiFe(5)/NiCu(5)/CoFe(5)/IrMn(10)/Ta(2) (magnetization occurs along the pinning axis); colored arrows show the passage direction along the magnet field. The schematic image of the specimen in a transverse section is shown on the inset; the black arrows indicate the compliance of the hysteresis loops with the FM layers, with the loops reflecting such remagnetization. (b) Experimental non-linear installation scheme.

The magneto-optic response of films has been investigated in the meridional magneto-optic Kerr effect (MOKE) scheme. In the case of double-layered films, loops of magnetic hysteresis of MOE are observed, symmetrical with respect to the zero value of the magnetic field ($H = 0$), coercivity is several dozen oersted. At the same time, in the case of the pinning structure of NiFe/NiCu/CoFe/IrMn/Ta, there is a more complex relationship (Fig. 1, a): there are two loops of magnetic hysteresis characterizing the shifting of NiFe and CoFe layers, and both loops are offset against the zero value of the external field to $H = 100\text{--}200$ Oe for NiFe and $H = 200\text{--}400$ Oe for CoFe. Dependencies of this kind, typical of pinning composite structures, have been observed before [2,4,6] and are associated with the exchange effects of ferromagnetic layers with the antiferromagnet [16,18].

Experiments on the generation of MWG were conducted in geometry to reflect or transmit in the Kerr equatorial effect scheme using p-polarized radiation of pulsed titanium-sapphire laser (generation wavelength 800 nm, pulse length ≈ 50 fs, average power from 24 mW to 50 mW, pulse rate 80 MHz); focused on the surface of the films in an area of about $30\ \mu\text{m}$; reflected or passed through the structure radiation at the frequency of VG was recorded by FEU; the incidence angle of probing radiation on the surface of the sample was 45° . The equatorial magnetic field up to 1.5 kOe was created by electromagnet.

3. Experimental results

In Fig. 2, a–c the dependence of the intensity of reflected VG on the stress of the external equatorial magnetic in the equatorial MOKE scheme for pinned structure NiFe/NiCu/CoFe/IrMn/Ta at different average pumping

power (40 mW, 34 mW, 28 mW) is shown, the pumping radiation was directed from the NiFe layer and magnetization was carried out along the pinning axis. There is one hysteresis loop in of these dependencies, shifted from $H = 0$ to the positive field stress range. To characterize the bias, the ratio of the areas of the hysteresis loops in the positive (S_+) and negative (S_-) magnetic field values for each of the three cases $W = 40, 34$ and 21 mW: $S_+/S_- = 1.7, 2.7$ and 21 , respectively. (see Fig. 2, a–c); this offset is similar to linear magneto-optic response, but it is much smaller and is about $|\Delta H| = 10, 25$ and 50 Oe, respectively. At the same time, there is no second hysteresis loop in the VG response.

Fig. 2, d presents the dependence of the intensity of VG on the stress of the external equatorial field, measured in geometry by the transmission at an average pumping power of 24 mW. As with the relationships for the reflected VG, there is only one hysteresis loop, offset against the zero field by about $|\Delta H| = 100$ Oe and located in the positive field.

To analyze the magnitude of the magneto-optic effect, a magnetic contrast of the intensity of VG was estimated in the response of VG, defined as

$$\rho_{2\omega} = \frac{I_{2\omega}(+H) - I_{2\omega}(-H)}{I_{2\omega}(+H) + I_{2\omega}(-H)},$$

where $I_{2\omega}(+H)$ and $I_{2\omega}(-H)$ — VG intensity for magnetic fields of different characters. For those in Fig. 2, a–c dependencies for pinning structure magnetic contrast VG is about $\rho_{2\omega} \approx -12\%$ for all four represented dependencies; at the same time when irradiating the structure on the opposite side the magnetic contrast VG had a reverse sign, that is expected in case of an inversion of the structure [13] and its absolute value for similar conditions of experiment exceeded 40%.

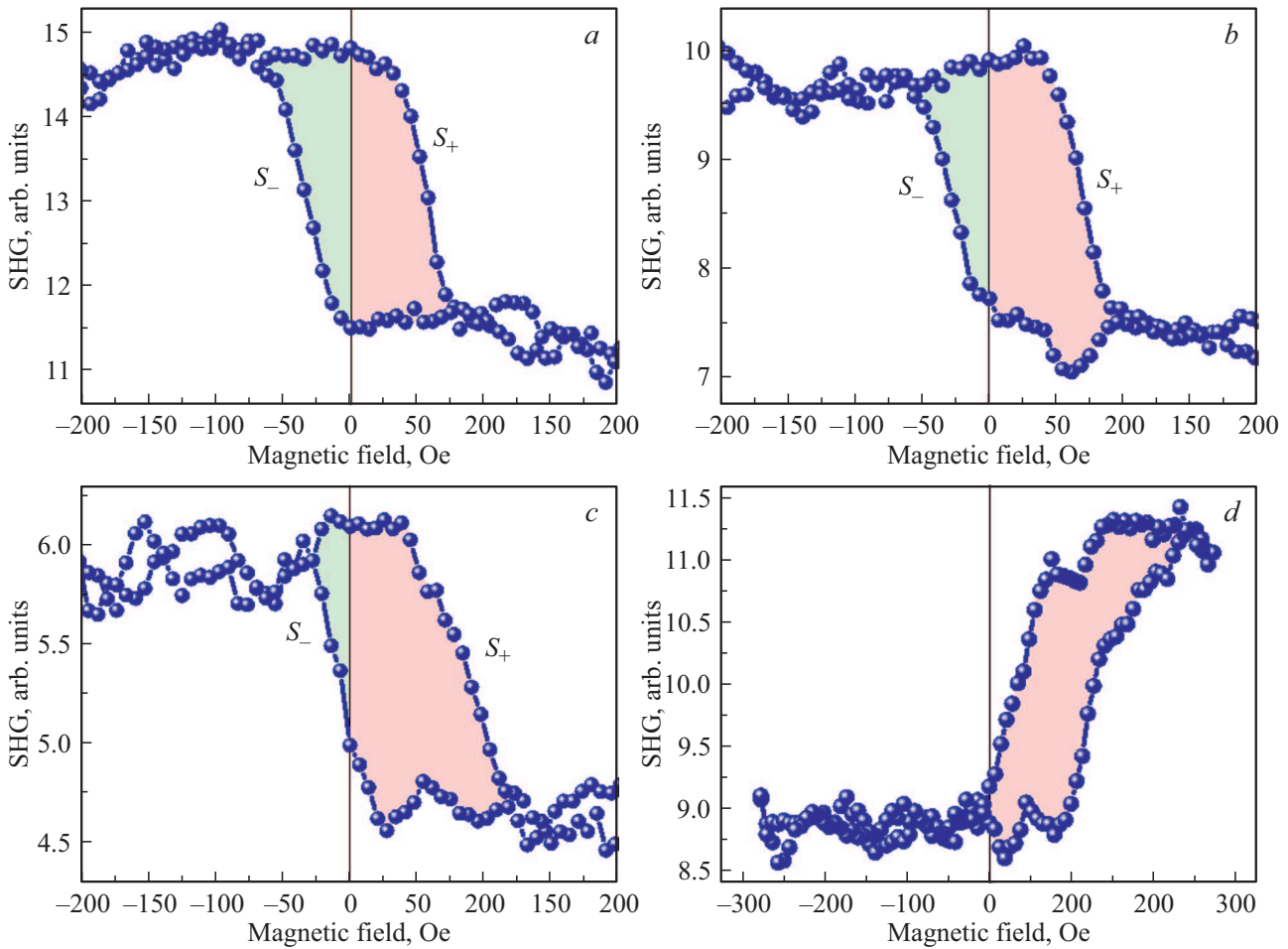


Figure 2. Dependence of VG intensity on equatorial external magnetic field for NiFe(5)/NiCu(5)/CoFe(5)/IrMn(10)/Ta(2) in geometry (a–c) by reflection and (d) by skipping; mean power of pumping was (a) 40 mW, (b) 34 mW, (c) 28 mW, (d) 24 mW. Magnetization occurs along the pinning axis. Pumping radiation incident angle of 45° .

Magnetic contrast values $\rho_{2\omega}$ for different interfaces; the order of writing corresponds to the order of probing radiation

Order of materials	NiFe/IrMn	IrMn/NiFe	NiFe/NiCu	NiCu/NiFe	CoFe/IrMn
$\rho_{2\omega}$	$-24 \pm 4\%$	$2 \pm 3\%$	$-18 \pm 3\%$	$18 \pm 3\%$	$22 \pm 2\%$

For comparison, a magneto-optic response to VG frequency was studied in double-layer films containing similar partition boundaries as in a multi-layer structure. Fig. 3, a–b shows VG intensity dependencies on external magnetic field for FM/AF CoFe(4)/IrMn(10) and NiFe(4)/IrMn(10) films; average pumping power was 50 mW; these films were applied to a crystalline silicon substrate, on top of them a protective layer of silicon of about 2 nm was applied, oxidized to silicon oxide. For double-layer films and the specified laser power, there is a slight shift of hysteresis loop relative to $H = 0$, much smaller than in the linear case (linear MOKE dependencies are represented in Fig. 3, c–d for CoFe(4)/IrMn(10) and NiFe(4)/IrM(10), respectively); the magnetic contrast is $\rho_{2\omega} \approx 22\%$ for CoFe/IrMn structure

and $\rho_{2\omega} \approx -24\%$ for NiFe/IrMn double-layer film. Similar measurements have been made for other double-layer films of different composition; the magnetic contrast values of VG intensity obtained are given in table.

4. Discussion of results

Let's discuss the results of the experimental study of VG generation in the described films. Note that, according to MOKE data, the ferromagnetic metal layers in the structure are exchange-bound. Since the materials of all layers in the studied structures are centrosymmetric, VG generation mainly occurs on the boundaries of the

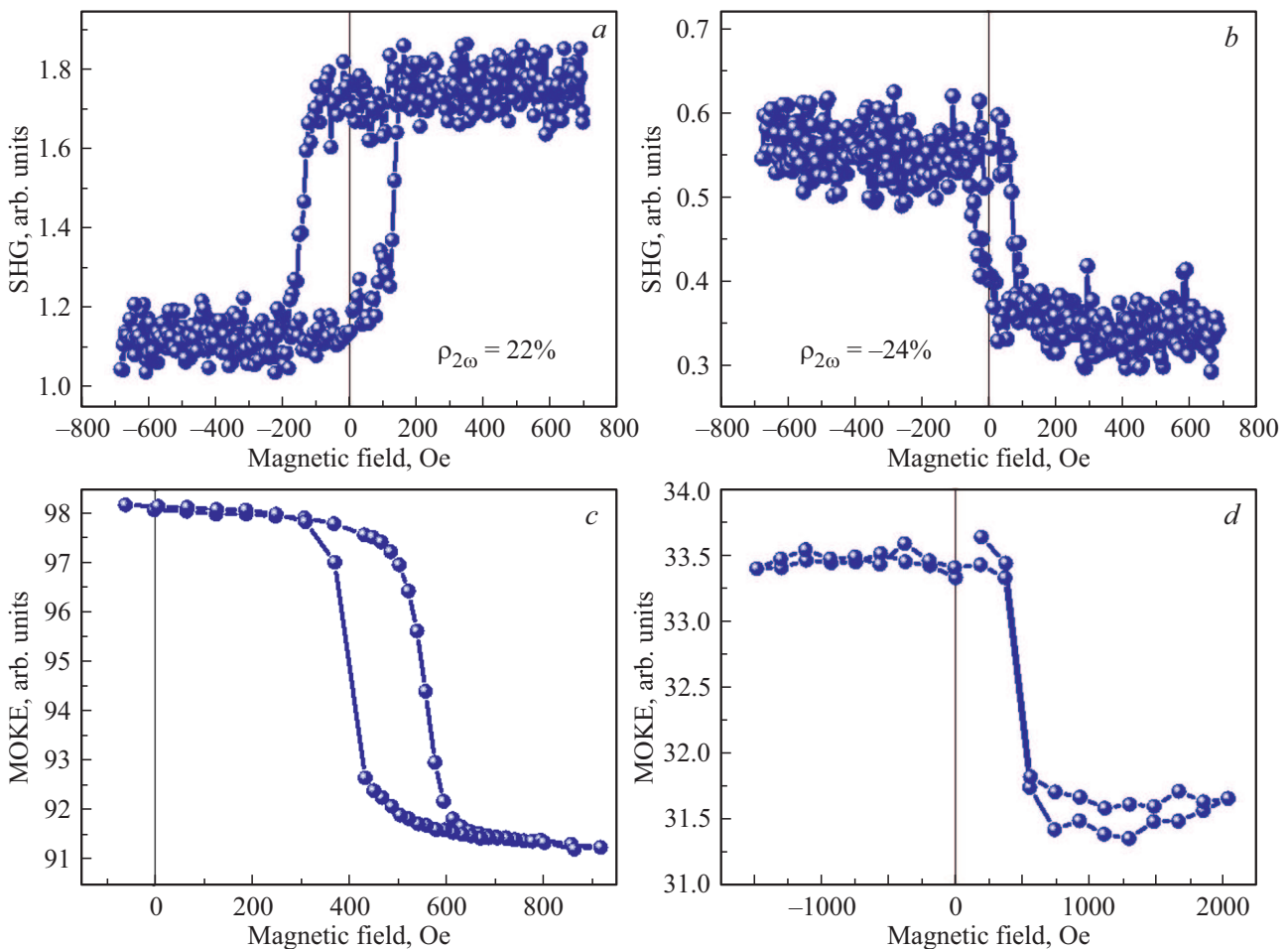


Figure 3. (a, b) The dependence of VG intensity on the equatorial external magnetic field and (c, d) linear MOKE for bilayered structures (a, c) CoFe(4)/IrMn(10) and (b, d) NiFe(4)/IrMn(10). The pumping inflation angle on the structure was 45°, power — 50 mW.

section, and their non-linear optical response is important for the formation of VG response from the whole film. It follows from the table that, depending on the material of the double-layer films, both the sign and the magnetic response at the frequency of VG may differ. The cumulative magnetic response on the WG frequency from the NiFe/NiCu/CoFe/IrMn/Ta multi-layer structure is formed by the deposits of all hidden magnetic interfaces; the difference in magnetic contrast of VG in reflection and transmission schemes is explained by the change of the normal direction to the film.

In contrast to linear magneto-optic response, the dependence of VG intensity on the external equatorial magnetic field exhibits one magnetic hysteresis loop, whose width is about 100 Oe, offset relative to the zero magnetic field value, the amount of this shift depends on the average amount of pumping radiation. By comparing the obtained parameters for VG dependence with the parameters of the hysteresis loops of the linear MOKE, it should be assumed that the observed non-linear response dependence is mainly related to the reversal of the pinning layer of CoFe. This

dependence can be superimposed on a similar for a free permalloy layer that has a narrower hysteresis loop.

As can be seen from the presented experimental relationships of the intensity of VG from the magnetic field, in the non-linear case, the asymmetry of the hysteresis loop decreases with the increase in the average intensity of the pumping. It can be assumed that the action of powerful pulsed laser radiation on the antiferromagnetic layer of IrMn reduces the effect of pinning. Planned additional experiments may clarify this hypothesis.

5. Conclusion

Thus, the paper studied the peculiarities of magneto-induced second harmonica generation in multi-layer films based on ferro-, para- and antiferromagnets: NiFe/NiCu/CoFe/IrMn/Ta, Si/CoFe/IrMn/Si and Si/NiFe/IrMn/Si, etc. It is shown that dependence of intensity of linear and nonlinear optical response on the intensity of the applied static magnetic field are different. In the first case, two magnetic hystereses are observed,

offset by a different value relative to the zero value of the magnetic field, associated with the magnetization of free and fixed ferromagnetic layers and reflecting the effects of exchange interaction in the structure. At the same time, there is only one hysteresis in the response of VG associated primarily with the scaling of the linked CoFe layer. The shear of this loop relative to the zero value of the magnetic field increases with a decrease in the pumping power, which is probably due to the degradation of pinning properties of the IrMn layer in the field of powerful laser radiation.

Funding

The work was carried out with the support of the Russian Science Foundation, grant No. 19-72-20103, using the equipment of CRC „Physics and Technology of micro- and nanostructures“ of IFM RAS, as well as the Foundation for the Development of Theoretical Physics and Mathematics BASIS grant No. 21-2-1-50-1).

Conflict of interest

The authors declare that they have no conflict of interest.

References

- [1] H. Yamamoto, T. Shinjo. IEEE Translat. J. Magn. Jpn **7**, 9, 674 (1992).
- [2] B. Dieny, V.S. Speriosu, S. Metin, S.S. P. Parkin, B.A. Gurney, P. Baumgart, D. Wilhoit. J. Appl. Phys. **69**, 4774 (1991).
- [3] I. Žutić, J. Fabian, S. Das Sarma. Rev. Mod. Phys. **76**, 323 (2004).
- [4] E.Y. Vedmedenko, R.K. Kawakami, D.D. Sheka, P. Gambardella, A. Kirilyuk, A. Hirohata, C. Binek, O. Chubykalo-Fesenko, S. Sanvito, B.J. Kirby, J. Grollier, K. Everschor-Sitte, T. Kampfrath, C.-Y. You, A. Berger. J. Phys. D **53**, 453001 (2020).
- [5] S. Yuasa, D.D. Djayaprawira. J. Phys. D **40**, R337 (2007).
- [6] I. Y. Pashenkin, M.V. Sapozhnikov, N.S. Gusev, V.V. Rogov, D.A. Tatarsky, A.A. Fraerman. ZhtF **89**, 11, 1732 (2019) (in Russian).
- [7] J. Bass, W.P. Pratt. J. Phys.: Condens. Matter **19**, 183201 (2007).
- [8] Spin Electronics/Eds M. Ziese, M.J. Thornton. Springer-Verlag, Berlin (2001).
- [9] R.Q. Zhang, J. Su, J.W. Cai, G.Y. Shi, F. Li, L.Y. Liao, F. Pan, C. Song. Appl. Phys. Lett. **114**, 092404 (2019).
- [10] Z.H. Xiong, Z.H. Xiong, Di Wu, Z. Vally Vardeny, Jing Shi. Nature **427**, 821 (2004)
- [11] R.-P. Pan, H.D. Wei, Y.R. Shen. Phys. Rev. B **39**, 1229 (1989).
- [12] J. Reif, C. Zink, C.M. Schneider, J. Kirschner. Phys. Rev. Lett. **67**, 2878 (1991).
- [13] A.K. Zvezdin, V.A. Kotov. Magnitooptika tonkikh plenok. Nauka, M. (1988). 192 s. (in Russian).
- [14] I.A. Kolmychek, V.V. Radovskaya, E.A. Mamonov, A.I. Mailykovskiy, A.V. Sadovnikov, S.E. Sheshukova, S.A. Nikitov, M.P. Temiryazeva, N.S. Gusev, A.A. Fraerman, T.V. Murzina. JMMM **528**, 167780 (2021).
- [15] T.V. Murzina, I.A. Kolmychek, N.S. Gusev, A.I. Mailykovskiy. Pis'ma v ZhETF **111**, 370 (2020) (in Russian).
- [16] V.K. Valev, M. Gruyters, A. Kirilyuk, Th. Rasing. Phys. Rev. Lett. **96**, 067206 (2006).
- [17] V.L. Krutyanskiy, I.A. Kolmychek, B.A. Gribkov, E.A. Karashtin, E.V. Skorohodov, T.V. Murzina. Phys. Rev. B **88**, 094424 (2013).
- [18] S.N. Vdovichev, N.I. Polushkin, I.D. Rodionov, V.N. Prudnikov, J. Chang, A.A. Fraerman. Phys. Rev. B **98**, 014428 (2018).

*The publication of conference papers
will be continued in No. 10/22*